Neutron matter calculations by the Fermi-hypernetted-chain method

B. Arntsen* and E. Østgaard

Fysisk Institutt, NLHT, Universitetet i Trondheim, 7055 Dragvoll, Norway
(Received 3 February 1984)

The Fermi-hypernetted-chain method for quantum many-body calculations is studied and investigated in some detail by calculations of the ground-state energy for neutron matter. The calculations are done for five different two-body potentials and results are compared with other theoretical results. Our Fermi-hypernetted-chain results are rather close to results obtained by lowest-order constrained variation calculations, and the results are quite dependent on the chosen potential, especially at high densities.

I. INTRODUCTION

Neutron matter is an infinite, homogeneous, and unpolarized system of interacting neutrons at densities $\rho \geq \rho_0$, where ρ_0 is the typical nuclear-matter particle density of nucleons in ordinary nuclei, i.e.,

$$\rho_0 \approx 0.17 \text{ fm}^{-3} \ . \tag{1.1}$$

One reason for studying such a system is that neutron stars are considered to consist, to a large extent, of neutrons at densities ranging from ρ_0 to $\rho \approx 20\rho_0$, and a first approximation to neutron star matter should be neutron matter. To calculate or estimate properties of neutron stars like mass, moment of inertia, luminosity, etc., we need an equation of state and the energy $E(\rho)$ for neutrons in the ground state. Neutron matter is also a useful test for quantum many-body theories, and relatively simple test models can be used to compare different methods numerically.

The most "probable" densities in neutron stars are in the range from ρ_0 up to $\rho \approx 3$ fm^{-3}. Neutron stars are assumed to have temperatures of the order of

$$T \approx 10^7 \text{ K} \ , \tag{1.2}$$

which corresponds to energies

$$E = kT \approx 100 \text{ keV} \ , \tag{1.3}$$

where k is Boltzmann's constant. The Fermi energy for a noninteracting neutron system at ρ_0 is

$$\epsilon_F \approx 40 \text{ MeV} \ , \tag{1.4}$$

and it follows that

$$(T/T_F) = (kT/\epsilon_F) \ll 1 \tag{1.5}$$

in a neutron star, i.e., the neutron system (liquid) can be considered to be (at zero temperature) in the ground state. For $\rho \approx \rho_0$ we also get

$$(E/mc^2) \ll 1 \ , \tag{1.6}$$

i.e., the system can be considered to be nonrelativistic, but for high densities we may get

$$(E/mc^2) \gtrsim 1 \ . \tag{1.7}$$

Some of the first energy calculations for neutron matter were done by Brueckner et al.[1] by their reaction matrix theory at small densities. They found that neutron matter is unbound, which has been confirmed by all later calculations. Binder et al.[2] obtained energy, pressure, and critical mass for neutron stars, and Østgaard[3] calculated neutron-matter energy and magnetic susceptibility for $\rho \leq 1.5$ fm^{-3}. Siemens and Pandharipande[4] used Brueckner theory and the lowest-order constrained variation (LOCV) method to calculate the energy $E(\rho)$ for 0.03 fm$^{-3} \leq \rho \leq 4.2$ fm^{-3}, with the Reid soft-core (RSC) potential. Schlenker and Lomon[5] used the Bressel-Kerman-Rouben (BKR) potential correspondingly for densities 0.02 fm$^{-3} \leq \rho \leq 0.3$ fm^{-3}. The first reliable variational calculations for high densities, however, were performed by Pandharipande and Bethe[6] in the Wu-Feenberg approximation, which gave approximately the same results as LOCV calculations, but they used only the central part of the RSC potential. Bethe and Johnson[7] constructed new and theoretically more satisfactory potentials, and the LOCV method then gave somewhat larger energies for the ground state and the RSC potential. Variational methods have been improved further after 1976 to include noncentral parts of the potentials in the calculations. Smith[8] included spin correlations, but obtained approximately the same results as Bethe and Johnson by their LOCV method. Later, Friedman and Pandharipande[9] have used a more "realistic" potential where tensor and spin-orbit terms are included. The energies then become considerably smaller than in the "old" RSC calculations, where only the central part of the RSC potential was included.

II. GENERAL THEORY

The energy in the ground state in the nonrelativistic limit is assumed to be given by

$$E = \langle \Psi | H | \Psi \rangle / \langle \Psi | \Psi \rangle \ , \tag{2.1}$$

where

$$H = - \sum_{i=1}^{N} (\hbar^2/2m)\nabla_i^2 + \sum_{i<j} v(r_{ij}) \ , \tag{2.2}$$

$| \psi \rangle$ is the ground-state wave function, $v(r_{ij})$ is the two-body potential corresponding to the interaction between

the neutrons, and m is the neutron mass. The "true" wave function will be determined by the two-body interaction potential, and a possible assumption for the total wave function of an N-body system is[10]

$$\Psi = \prod_{1 \le i < j \le N} f(r_{ij}) \Phi(\vec{x}_1, \ldots, \vec{x}_N)$$

$$= \prod_{1 \le i < j \le N} f(r_{ij}) |\Phi\rangle = |\Psi\rangle , \qquad (2.3)$$

which should be antisymmetric and "physically acceptable."

We want to consider a "power series" (PS) expansion for the energy, which is a systematic expansion in powers of density and integrals of the functions

$$h(r) = f^2(r) - 1 \qquad (2.4)$$

and the Slater functions

$$L(k_F r) = 3(k_F r)^{-3} [\sin(k_F r) - k_F r \cos(k_F r)] . \qquad (2.5)$$

The energy can then be expressed by the PS expansion, but the convergence of the expansion will depend on the density and the functions $h(r)$ and $L(k_F r)$. We would normally expect fast convergence for low density or when $f(r) \to 1$ relatively fast with increasing r, i.e., for a short "healing" distance. Calculations where only a few terms of the PS expansion are included have been tried for many different many-body systems,[6,11-16] where $f(r)$ is chosen to give a fast convergence of the PS expansion.

Pandharipande, for instance, has suggested a method of lowest-order constrained variation,[11,12] where only the first term (the "two-body cluster") is kept in the PS expansion, and certain boundary conditions or healing conditions are included for $f(r)$. The LOCV method is a relatively fast and simple method for calculating physical quantities like the binding energy of many-body systems.[17] But it is not a purely variational method since it requires the additon of a parameter λ to the interaction potential, and in some cases it gives poorer results than other methods.[18] The main virtue of the LOCV method, therefore, seems to be the simplicity of the calculations.

The most important assumption in the LOCV method is that the PS expansion can be neglected after the first term, but this is not well founded on theoretical grounds. To include higher-order terms, we want to consider the Fermi hypernetted-chain (FHNC) method, which is developed analogously to the hypernetted-chain (HNC) method for classical gases.[19] In one version of the FHNC method,[20] which is probably best for long-range interactions, certain systematic cancellations between terms are included, but relatively few terms are summed over (included) at the end. In another version of the FHNC method,[21] which is probably best for short-range interactions, more terms are included in the final expressions.

To sum all the terms in the PS expansion we use a diagram representation, i.e., we consider irreducible diagrams only, since reducible diagrams cancel out. Each diagram can be factorized into simple diagrams, and simple diagrams are nodal diagrams or elementary diagrams. All elementary diagrams can be obtained from basic diagrams

by replacing simple connections by summation of all types of (nodal and non-nodal) diagrams.[23]

A possible way to obtain the sum of all diagrams in the FHNC method then would be to choose the correlation function $f(r)$, set all sums of elementary diagrams equal to zero, solve the FHNC equations, calculate the sum of elementary diagrams obtained from basis diagrams and sums of all (nodal and non-nodal) diagrams, and go back and iterate through the same procedure until we get convergence. The main problem here is to calculate the sum of elementary diagrams, and this sum is generally approximated by some basic diagrams with just a few internal points. The simplest approximation would be to set the sum equal to zero, i.e., we get the FHNC/0 approximation. If we classify diagrams according to how many points enter in the basic diagrams included, we get a (FHNC/n) expansion where FHNC/0 is the "lowest-order" approximation where no basic diagrams are included.[23]

We may now assume that the FHNC/0 approximation should give a useful first approximation to the ground-state energy, but there may be some cancellation between elementary and nodal diagrams because of the antisymmetry of the wave functions.[20] For short-range interactions and for liquid ^{3}He, however, the FHNC/0 approximation seems to work reasonably well as a first approximation.[22]

III. THE FHNC/0 APPROXIMATION

The FHNC method, and the FHNC/0 approximation in neutron-matter calculations, have been outlined and explained in detail earlier,[23] so we will here simply give the equations to be solved in our method. We may choose a trial function $\Psi(d)$ to be varied to give a minimum value for the energy (2.1), i.e.,

$$E = \langle \Psi(d) | H | \Psi(d) \rangle / \langle \Psi(d) | \Psi(d) \rangle , \qquad (3.1)$$

where d is a healing distance for the wave function.

We first calculate the correlation function $f(r)$, i.e., in the LOCV method, $f_l(r)$ should satisfy the equation[17]

$$f_l'' + 2f_l' J_l'(k_{av}r)/J_l(k_{av}r) - (m/\hbar^2)(v_l + \lambda_l)f_l = 0 , \qquad (3.2)$$

where

$$J_l(k_{av}r) = k_{av}r j_l(k_{av}r) ,$$
$$k_{av} = \sqrt{0.3}k_F = \sqrt{0.3}(3\pi^2\rho)^{1/3} , \qquad (3.3)$$

$j_l(kr)$ are spherical Bessel functions, and the boundary conditions are

$$f_l(0) = 0 ,$$
$$f_l(d) = 1 , \qquad (3.4)$$
$$f_l'(d) = 0 .$$

It seems to be a good approximation to use such a correlation function as an input in our FHNC calculations.[24]

We also calculate the functions[23]

$$f_{\mathrm{av}}^2(r) = \{[1 + L^2(k_f r)]f_0^2(r) + 3[1 - L^2(k_F r)]f_1^2(r) + T(k_F r)[f_0^2(r) - f_2^2(r)]\}/4[1 - \tfrac{1}{2}L^2(k_F r)] \,, \tag{3.5}$$

$$\begin{aligned}
f_{\mathrm{av}}'(r)/f_{\mathrm{av}}(r) = \{&[1 + L^2(k_F r)]f_0(r)f_0'(r) + 3[1 - L^2(k_F r)]f_1(r)f_1'(r) \\
&+ T(k_F r)[f_0(r)f_0'(r) - f_2(r)f_2'(r)]\}/\{4f_{\mathrm{av}}^2(r)[1 - \tfrac{1}{2}L^2(k_F r)]\} \,,
\end{aligned}$$

where $L(k_F r)$ is given by (2.5), and

$$T(k_F r) = 9(k_F r)^{-6}\{(k_F r)^4 - (k_F r)^2[1 + \cos^2(k_F r)] + 4k_F r \sin(k_F r)\cos(k_F r) - 2\sin^2(k_F r)\} - 1 \,. \tag{3.6}$$

Sums of nodal diagrams are represented by the functions[23] $G_{ss}(r_{ij})$, $G_{sh}(r_{ij})$, $G_{hh}(r_{ij})$, and $G_{dd}(r_{ij})$, and sums of elementary diagrams are represented by the functions $E_{ss}(r_{ij})$, $E_{sh}(r_{ij})$, $E_{hh}(r_{ij})$, and $E_{dd}(r_{ij})$. For

$$E_{ss} = E_{sh} = E_{hh} = E_{dd} = 0 \,, \tag{3.7}$$

we solve the integral equations

$$G_{ss}(r_{12}) = \rho \int [G_{ss}(r_{12}) + \alpha(r_{13})]p(r_{23})d^3r_3 \,,$$

$$G_{sh}(r_{12}) = \rho \int \{\alpha(r_{12})\beta(r_{23}) - \gamma(r_{13})\gamma(r_{23}) + [G_{sh}(r_{13}) + \gamma(r_{13})]p(r_{23})\}d^3r_3 \,,$$

$$G_{hh}(r_{12}) = \rho \int \{\gamma(r_{13})\gamma(r_{23}) - \alpha(r_{13})\beta(r_{23}) + [G_{hh}(r_{13}) + \beta(r_{13})]p(r_{23})\}d^3r_3 \,,$$

$$G_{dd}(r_{12}) = \rho \int \delta(r_{13})[G_{dd}(r_{23}) + \delta(r_{23}) - \tfrac{1}{2}L(k_F r_{23})]d^3r_3 \,,$$

$$\tag{3.8}$$

where

$$\alpha(r_{ij}) = f_{\mathrm{av}}^2(r_{ij})\exp[G_{ss}(r_{ij})] - G_{ss}(r_{ij}) - 1 \,,$$

$$\beta(r_{ij}) = f_{\mathrm{av}}^2(r_{ij})[G_{hh}(r_{ij}) + G_{sh}^2(r_{ij}) - 2G_{dd}^2(r_{ij}) + 2L(k_F r_{ij})G_{dd}(r_{ij}) - \tfrac{1}{2}L^2(k_F r_{ij})]\exp[G_{ss}(r_{ij})] - G_{hh}(r_{ij}) \,,$$

$$\gamma(r_{ij}) = f_{\mathrm{av}}^2(r_{ij})G_{sh}(r_{ij})\exp[G_{ss}(r_{ij})] - G_{sh}(r_{ij}) \,,$$

$$\tag{3.9}$$

$$\delta(r_{ij}) = f_{\mathrm{av}}^2(r_{ij})[G_{dd}(r_{ij}) - \tfrac{1}{2}L(k_F r_{ij})]\exp[G_{ss}(r_{ij})] + \tfrac{1}{2}L(k_F r_{ij}) - G_{dd}(r_{ij}) \,,$$

$$p(r_{ij}) = \alpha(r_{ij}) + 2\gamma(r_{ij}) + \rho \int [\alpha(r_{ik})\beta(r_{jk}) - \gamma(r_{ik})\gamma(r_{jk})]d^3r_k \,.$$

The energy per particle is calculated as[23]

$$E/N = \epsilon_F + W + W_F + U + U_F \,, \tag{3.10}$$

where

$$\epsilon_F = \tfrac{3}{10}(\hbar^2/m)(3\pi^2\rho)^{2/3} \,,$$

$$W + W_F = \tfrac{1}{8}\rho \int d^3r \left[\sum_{s=0}^{1} \bar{v}_s^{\mathrm{eff}} g_s(r_{12}) \right] \,,$$

$$\tag{3.11}$$

$$\begin{aligned}
U = -4\pi^2\rho^2(\hbar^2/m) \int_0^\infty r_{12}^2[f_{\mathrm{av}}'(r_{12})/f_{\mathrm{av}}(r_{12})]dr_{12} \int_0^\infty r_{13}^2[f_{\mathrm{av}}'(r_{13})/f_{\mathrm{av}}(r_{13})]dr_{13} \\
\times \int_{-1}^{1} d(\cos\theta_{12})\cos\theta_{12}g_3(r_{12},r_{13},\cos\theta_{12}) \,,
\end{aligned}$$

$$\begin{aligned}
U_F = -8\pi^2\rho^2(\hbar^2/m) \int_0^\infty r_{12}^2[f_{\mathrm{av}}'(r_{12})/f_{\mathrm{av}}(r_{12})]dr_{12} \int_0^\infty r_{13}^2 L'(k_F r_{13})dr_{13} \\
\times \int_{-1}^{1} d(\cos\theta_{12})\hat{g}_3(r_{12},r_{13},\cos\theta_{12})\cos\theta_{12} \,.
\end{aligned}$$

Here

$$\bar{v}_0^{\mathrm{eff}} = \bar{v}_{\mathrm{even}\,l}^{\mathrm{eff}} = v_{l=0}^{\mathrm{eff}} + (v_{l=0}^{\mathrm{eff}} - v_{l=2}^{\mathrm{eff}})T(k_F r_{12})/[1 + L^2(k_F r_{12})] \,,$$

$$\bar{v}_1^{\mathrm{eff}} = \bar{v}_{\mathrm{odd}\,l}^{\mathrm{eff}} = v_{l=1}^{\mathrm{eff}} \,,$$

$$g_s(r_{12}) = (2s + 1)[1 + (-1)^s L^2(k_F r_{12})]H(r_{12}) + H_1(r_{12}) - (-1)^s H_{1,\mathrm{ex}}(r_{12}) \,,$$

$$\begin{aligned}
g_3(r_{12},r_{13},r_{23}) = \bar{L}_{ss}(r_{12})\bar{L}_{ss}(r_{13})\bar{L}_{ss}(r_{23}) + 2 \\
\times [L_{sh}(r_{12})\bar{L}_{ss}(r_{13})\bar{L}_{ss}(r_{23}) + L_{sh}(r_{13})\bar{L}_{ss}(r_{12})\bar{L}_{ss}(r_{23}) + L_{sh}(r_{23})\bar{L}_{ss}(r_{12})\bar{L}_{ss}(r_{13})] \\
+ 3[L_{sh}(r_{12})\bar{L}_{ss}(r_{23})L_{sh}(r_{12}) + L_{sh}(r_{12})\bar{L}_{ss}(r_{13})L_{sh}(r_{23}) \\
+ L_{sh}(r_{13})\bar{L}_{ss}(r_{12})L_{sh}(r_{23})] + 2L_{sh}(r_{12})L_{sh}(r_{13})L_{sh}(r_{23})
\end{aligned}$$

$$+2[L_{hh}(r_{13})\bar{L}_{ss}(r_{12})L_{sh}(r_{23})+\bar{L}_{ss}(r_{13})L_{hh}(r_{23})L_{sh}(r_{12})+L_{hh}(r_{12})L_{sh}(r_{13})\bar{L}_{ss}(r_{23})]$$

$$+\bar{L}_{ss}(r_{12})\bar{L}_{ss}(r_{23})L_{hh}(r_{13})+L_{hh}(r_{23})\bar{L}_{ss}(r_{12})\bar{L}_{ss}(r_{13})+L_{hh}(r_{12})\bar{L}_{ss}(r_{13})\bar{L}_{ss}(r_{23})$$

$$-2sL_{dd}(r_{12})L_{dd}(r_{23})L_{dd}(r_{13}) ,$$

(3.12)

$$L'(k_Fr)=d[L(k_Fr)]/dr=(3/k_Fr^2)[\sin(k_Fr)-k_FrL(k_Fr)] ,$$

$$\hat{g}_3(r_{12},r_{13},r_{23})=\bar{L}_{ss}(r_{13})F_1(r_{13})\bar{L}_{ss}(r_{12})[\bar{L}_{ss}(r_{23})-1+\bar{L}_{ss}(r_{23})G_{sh}(r_{23})]$$

$$+\bar{L}_{ss}(r_{13})\bar{L}_{ss}(r_{12})F_1(r_{12})[\bar{L}_{ss}(r_{23})-1]F_1(r_{23}) ,$$

where

$$H(r_{12})=\exp[G_{ss}(r_{12})] ,$$

$$H_1(r_{12})=[2G_{sh}(r_{12})+G_{sh}^2(r_{12})+G_{hh}(r_{12})]\exp[G_{ss}(r_{12})] ,$$

$$H_{1,ex}(r_{12})=4[L_{ss}(k_Fr_{12})G_{dd}(r_{12})-G_{dd}^2(r_{12})]\exp[G_{ss}(r_{12})] ,$$

$$F_1(r)=-\tfrac{1}{2}L(k_Fr)+G_{dd}(r) ,$$

(3.13)

$$\bar{L}_{ss}(r)=f_{av}^2(r)\exp[G_{ss}(r)] ,$$

$$L_{hh}(r)=f_{av}^2(r)[G_{hh}(r)+G_{sh}^2(r)-2G_{dd}^2(r)+2L(k_Fr)G_{dd}(r)-\tfrac{1}{2}L^2(k_Fr)]\exp[G_{ss}(r)] ,$$

$$L_{sh}(r)=f_{av}^2(r)G_{sh}(r)\exp[G_{ss}(r)] ,$$

$$L_{dd}(r)=f_{av}^2(r)[G_{dd}(r)-\tfrac{1}{2}L(k_Fr)]\exp[G_{ss}(r)] .$$

For comparison, we may also calculate the energy in the LOCV approximation, where we use the healing condition[25]

$$\rho\omega(d)=1 ,$$

(3.14)

where

$$\omega(d)=\omega_0(d)+\omega_1(d)+\pi\int_0^d[f_0^2(r)-f_2^2(r)]T(k_Fr)r^2dr ,$$

$$\omega_0(d)=\pi\int_0^d f_0^2(r)[1+L^2(k_Fr)]r^2dr ,$$

(3.15)

$$\omega_1(d)=3\pi\int_0^d f_1^2(r)[1-L^2(k_Fr)]r^2dr .$$

The energy is then given by[25]

$$E_{LOCV}/N=\epsilon_F+\tfrac{1}{2}\pi\rho\int_0^\infty r^2dr\{v_0^{eff}[1+L^2(k_Fr)]+3v_1^{eff}[1-L^2(k_Fr)]+(v_0^{eff}-v_2^{eff})T(k_Fr)\}$$

$$=\tfrac{3}{10}(\hbar^2/m)(3\pi^2\rho)^{2/3}-\tfrac{1}{2}\rho\left\{\lambda_0\omega_0(d)+\lambda_1\omega_1(d)+\pi\int_0^d[\lambda_0 f_0^2(r)-\lambda_2 f_2^2(r)]T(k_Fr)r^2dr\right\}$$

(3.16)

$$+\tfrac{1}{2}\pi\rho\int_d^\infty\{v_0(r)[1+L^2(k_Fr)]+3v_1(r)[1-L^2(k_Fr)]+[v_0(r)-v_2(r)]T(k_Fr)\}r^2dr ,$$

when

$$v_l^{eff}=\begin{cases}-\lambda_l f_l^2, & \text{for } r\leq d , \\ v_l, & \text{for } r>d ,\end{cases}$$

(3.17)

d is the healing distance, and f_l should satisfy (3.2).

IV. NUCLEON-NUCLEON POTENTIALS

The energy is calculated for four different potentials, which are assumed to be local and static, but different for states of different isospin T, spin S, orbital angular momentum L, or angular momentum J. Neutron matter has total isospin $T=1$, and the neutron-neutron interactions show a strong exchange character, i.e., a great difference between odd-L and even-L state potentials, but otherwise a weak L dependence. Potentials of different forms generally give different results for the energy calcu-

lations, and the strongly repulsive short-range part of the potential can be very important for calculations at high densities.

At relative distances greater than 3 fm, the nucleon-nucleon interaction should be dominated by the one-pion-exchange potential

$$V^{OPEP}=\tfrac{1}{12}g^2 m_\pi c^2(m_\pi/m_n)^2\vec{\tau}_1\cdot\vec{\tau}_2$$

$$\times[\vec{\sigma}_1\cdot\vec{\sigma}_2+S_{12}(1+3x^{-1}+3x^{-2})]x^{-1}\exp(-x) ,$$

(4.1)

where m_π is the pion mass, m_n is the nucleon mass, the tensor operator S_{12} is

$$S_{12}=3(\vec{\sigma}_1\cdot\vec{r})(\vec{\sigma}_2\cdot\vec{r})-\vec{\sigma}_1\cdot\vec{\sigma}_2 ,$$

(4.2)

and

$$x = (m_\pi c / \hbar) r \; ,$$

$$g^2 \approx 14 \; . \tag{4.3}$$

At shorter distances, the nucleon-nucleon potential is represented by sums of Yukawa potentials of the form $x^{-1}\exp(-nx)$, where n is an integer. Hard or soft cores represent the strong short-range repulsion because of meson exchange.

The Hamada-Johnston (HJ) potential[26] is defined by

$$V(r) = V_c(r) + V_T(r)S_{12} + V_{LS}(r)(\vec{L}\cdot\vec{S}) + V_{LL}(r)L_{12} \; , \tag{4.4}$$

where V_c, V_T, V_{LS}, and V_{LL} are central, tensor, linear

spin-orbit, and quadratic spin-orbit potentials, and the quadratic spin-orbit operator L_{12} is defined by

$$L_{12} = [\delta_{LJ} + (\vec{\sigma}_1 \cdot \vec{\sigma}_2)]\vec{L}^2 - (\vec{L}\cdot\vec{S})^2 \; . \tag{4.5}$$

The noncentral components of the triplet-odd interaction are not important in energy calculations[27] and can be neglected. We finally get a potential with a hard core of radius

$$r_c = 0.4855 \text{ fm} \tag{4.6}$$

in all states, represented by a potential of 10^5 MeV for $r \leq r_c$ in our numerical calculations, and a neutron-neutron interaction given, for $r > r_c$, by

$$V(S=0) = V_0 = -15.931 r^{-1}\exp(-0.7r) - 198.005 r^{-2}\exp(-1.4r) - 344.639 r^{-3}\exp(-2.1r) \; ,$$

$$V(S=1) = V_1 = 5.310 r^{-1}\exp(0.7r) - 68.809 r^{-2}\exp(-1.4r) + 37.715 r^{-3}\exp(-2.1r) \; , \tag{4.7}$$

in MeV when r is given in fm.

For the Reid soft-core (RSC) potential[28] we use the $^1D_2$ central potential for all even-$L\neq0$ states, and we use the central part of the P-state potential for all odd-L states, which we again represent by the $V_c(^3P_2\text{-}^3F_2)$ potential since energy calculations seem to indicate that this is a good approximation for average densities, i.e., the potential is given by

$$V(S=0,L=0) = V_0 = -14.947 r^{-1}\exp(-0.7r) - 2358.0 r^{-1}\exp(-2.8r) + 9263.1 r^{-1}\exp(-4.9r) \; ,$$

$$V(S=0,\text{even } L \geq 2) = V_2 = -14.947 r^{-1}\exp(-0.7r) - 17.603 r^{-1}\exp(-1.4r)$$

$$- 1589.4 r^{-1}\exp(-2.8r) + 9263.1 r^{-1}\exp(-4.9r) \; , \tag{4.8}$$

$$V(S=1,\text{odd } L) = V_c(^3P_2\text{-}^3F_2) = 4.982 r^{-1}\exp(-0.7r) - 1333.54 r^{-1}\exp(-2.8r) + 5931.6 r^{-1}\exp(-4.2r) \; ,$$

in MeV when $\vec{r}$ is given in fm.

The hard core in the Hamada-Johnston potential is replaced by finite square wells in the Bressel-Kerman-Rouben (BKR) soft-core potential,[29] which is defined by

$$V(\text{singlet even}) = V(\text{triplet odd}) = 670 \text{ MeV} \; , \tag{4.9}$$

for $r \leq r_c$, where

$$r_c = 0.6983 \text{ fm} \approx 0.7 \text{ fm} \; . \tag{4.10}$$

For $r > r_c$, we get

$$V(S=0,\text{even } L) = -15.670 r^{-1}\exp(-0.7r) - 194.92 r^{-2}\exp(-1.4r) - 338.978 r^{-3}\exp(-2.1r) \; ,$$

$$V(S=1,\text{odd } L) = 5.223 r^{-1}\exp(-0.7r) - 83.572 r^{-2}\exp(-1.4r) + 34.964 r^{-3}\exp(-2.1r) \; , \tag{4.11}$$

when noncentral components are neglected.

Bethe and Johnson[7] have constructed several potentials where hard or soft cores represent the strong short-range repulsion because of ω and ρ meson exchange. The simplest potential is their model-I potential which is constructed by using the RSC potential (4.8) for all even-L states. For odd-L states, the potential is

$$V(S=1,\text{odd } L) = 4.982 r^{-1}\exp(-0.7r) - 32.56 r^{-1}\exp(-1.4r) - 528.57 r^{-1}\exp(-2.8r) + 9262.86 r^{-1}\exp(-4.9r) \; , \tag{4.12}$$

in MeV when r is given in fm.

A convenient potential for comparing different many-body methods and calculations is a simple Yukawa-type potential, suggested by Bethe and defined as

$$V_1 = 9263.1 r^{-1}\exp(-4.9r) \; , \tag{4.13}$$

which corresponds to the repulsive part of the Reid soft-core $V(S=0,L=0)$ potential. This potential is used, for instance, for comparison with Monte Carlo calculations.

V. CALCULATIONS AND RESULTS

The total binding energy E/N per particle for neutron matter is now calculated by the LOCV method and the FHNC/0 method for the different potentials, with

$$m_n c^2 = 939.573 \text{ MeV} ,$$

$$\hbar^2/m_n = 41.443 \text{ MeV fm}^2 ,$$

(5.1)

where m_n is the neutron mass, c is the speed of light, and $\hbar$ is Planck's constant. In both methods we have to solve (3.2) with the boundary conditions (3.4), and we need

$$J_0'(kr)/J_0(kr) = k \cot(kr) ,$$

$$J_1'(kr)/J_1(kr) = k\{kr/[1 - kr \cot(kr)] - (kr)^{-1}\} ,$$

$$J_2'(kr)/J_2(kr) = r^{-1}\{6kr - (kr)^3 + [3(kr)^2 - 6]tg(kr)\}/\{[3 - (kr)^2]tg(kr) - 3kr\} .$$

(5.2)

The differential equation (3.2) is solved by the Runge-Kutta-Nyström method[17,25] for $l = 0$, 1, and 2. It is a general method for solving second order differential equations and it is correct to fourth order in the Taylor expansion for y and y' when we, in general, have a second order problem

$$y'' = f(x,y,y') ,$$

(5.3)

with the boundary conditions

$$y(x_0) = y_0 ,$$

$$y'(x_0) = y_0' .$$

(5.4)

Assuming that $f(x,y,y')$ has a unique solution in some interval containing x_0, we can find the solution by Taylor expansions for y and y'.[17,25] In the calculations we have a self-consistency problem from the beginning because $\lambda_l(\rho)$ is not known, but at the same time ρ enters the equations explicitly. The procedure, therefore, becomes as shown in Fig. 1 for the LOCV method.

The integral equations in the FHNC method contain two-dimensional integrals of the type

$$Z(|\vec{r}_1 - \vec{r}_2|) = \rho \int x(|\vec{r}_3 - \vec{r}_1|)y(|\vec{r}_3 - \vec{r}_2|)d^3r_3 ,$$

(5.5)

which can be rewritten[22]

$$Z(r_{12}) = 8\rho \int_0^\infty k^2 dk \int_0^\infty r_a^2 dr_a \int_0^\infty r_b^2 dr_b y(r_a) x(r_b) j_0(kr_{12}) j_0(kr_a) j_0(kr_b) ,$$

(5.6)

by the convolution theorem. Numerically, we have to calculate the integrals as

$$Z(r_{12}) = 8\rho \int_0^\infty k^2 j_0(kr) \left[\sum_{j=1}^N y(r_j) j_0(kr_j)\omega_j r_j^2 \right] \left[\sum_{i=1}^N x(r_i) j_0(kr_i)\omega_i r_i^2 \right]$$

$$= 8\rho \int_0^\infty \sum_{i=1}^N \sum_{j=1}^N r_{12}^{-1} r_i r_j y(r_j) x(r_i)\omega_i\omega_j \int_0^\infty k^{-1} dk \sin(kr_i)\sin(kr_j)\sin(kr_{12}) .$$

(5.7)

The last integration can be performed as

$$\int_0^\infty k^{-1}\sin(kr_i)\sin(kr_j)\sin(kr_{12})dk = \frac{1}{4}\int_0^\infty k^{-1}dk[\sin(Ak) + \sin(Bk) + \sin(Ck) - \sin(Dk)]$$

$$= \frac{1}{8}\pi[\text{sgn}(A) + \text{sgn}(B) + \text{sgn}(C) - \text{sgn}(D)] ,$$

(5.8)

where

$$A = r_i - r_j + r_{12} ,$$

$$B = r_j + r_{12} - r_i ,$$

$$C = r_i + r_j - r_k ,$$

$$D = r_i + r_j + r_k ,$$

(5.9)

$$\text{sgn}(x) = \begin{cases} +1, & \text{for } x > 0 , \\ 0, & \text{for } x = 0 , \\ -1, & \text{for } x < 0 , \end{cases}$$

i.e.,

$$Z(r_k) = \rho\pi \sum_{i=1}^N \sum_{j=1}^N x(r_i)y(r_j)[\text{sgn}(A) + \text{sgn}(B) + \text{sgn}(C) - 1]r_i r_j r_k^{-1}\omega_i\omega_j$$

$$= \rho\pi r_k^{-1} \left[\sum_{i=1}^N I_a(r_i) + I_b(r_i) + I_c(r_i) + I_d(r_i) \right] ,$$

(5.10)

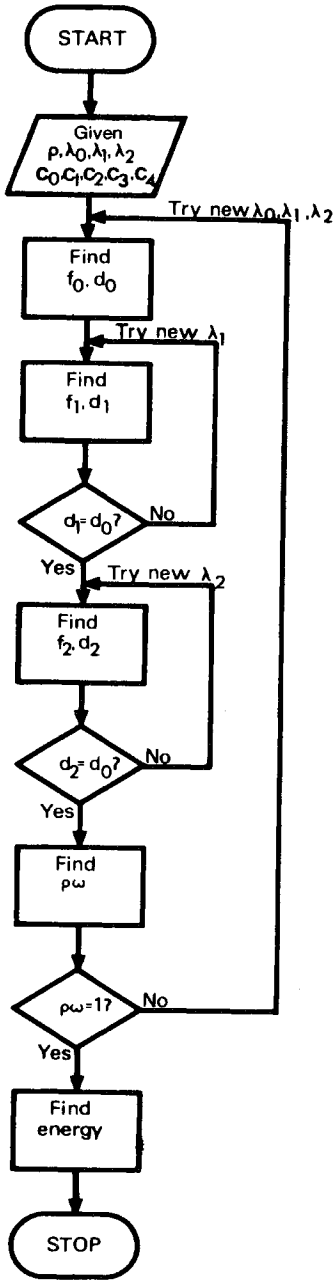FIG. 1. The scheme of calculations for the LOCV method.

FIG. 2. The scheme of calculations for the FHNC/0 method.

where

$$I_a = x(r_i)r_i\omega_i[T_{i+k-1} - (T_N - T_{i+k})] \ ,$$

$$I_b = \begin{cases} x(r_i)r_i\omega_i T_N, & \text{for } i \leq k \ , \\ x(r_i)r_i\omega_i(T_N - T_{i-k} - T_{i-k-1}), & \text{for } i > k \ , \end{cases}$$
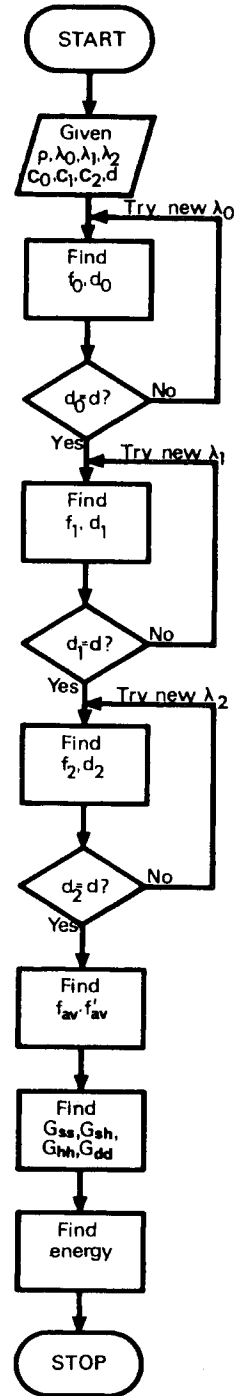
$$(5.11)$$

$$I_c = \begin{cases} x(r_i)r_i\omega_i(T_N - T_{k-i} - T_{k-i-1}), & \text{for } i < k \ , \\ x(r_i)r_i\omega_i T_N, & \text{for } i \geq k \ , \end{cases}$$

$$I_d = x(r_i)r_i\omega_i T_N \ ,$$

$$T_m = \sum_{j=1}^{m} y(r_j)r_j\omega_j \ .$$

B. ARNTSEN AND E. ØSTGAARD

TABLE I. Binding energy of neutron matter calculated with the Hamada-Johnston potential.

ρ (fm^{-3})	$E_2^{(0)}$ (MeV)	$E_2^{(1)}$ (MeV)	T_3 (MeV)	E_{HO} (MeV)	ϵ_F (MeV)	E/N (MeV)
0.4	−35.2	−4.4	3.7	−0.8	64.6	28.6
0.6	−38.8	−0.6	10.1	9.5	84.7	55.4
0.8	−39.0	−4.8	32.7	27.9	102.5	91.4
1.0	−33.1	2.2	58.4	60.6	119.0	146.5
1.1	−29.6	7.9	75.4	83.3	126.8	180.5
1.4	−12.3	32.6	150.9	183.6	148.9	320.1

TABLE II. Binding energy of neutron matter calculated with the Reid soft-core potential.

ρ (fm^{-3})	$E_2^{(0)}$ (MeV)	$E_2^{(1)}$ (MeV)	T_3 (MeV)	E_{HO} (MeV)	ϵ_F (MeV)	E/N (MeV)
0.2	−19.0	−2.2	0.6	−1.6	40.7	19.5
0.4	−25.3	−3.7	4.8	1.1	64.6	39.8
0.6	−21.8	−2.1	11.6	9.5	84.7	70.0
0.8	−12.3	4.8	20.2	25.0	102.5	110.1
1.0	1.5	14.2	30.3	44.5	119.0	156.4
1.2	7.5	25.4	43.2	68.6	134.4	210.5
1.4	28.0	40.2	54.3	94.5	148.9	271.4
1.6	50.5	57.0	66.2	123.2	162.8	336.5
1.8	77.0	74.6	78.3	152.9	176.1	406.0
2.0	107.6	98.0	86.9	184.9	188.9	481.4
2.2	142.8	118.2	101.8	219.9	201.3	564.0
2.4	178.3	146.5	109.1	255.6	213.3	647.2
2.6	218.8	164.6	125.3	289.8	225.0	733.6
2.8	261.6	196.8	131.3	328.1	236.4	826.1
3.0	304.3	213.2	149.5	362.7	247.5	914.5
3.2	353.1	248.2	155.4	403.5	258.4	1015.0
3.4	406.2	258.7	173.8	432.5	269.1	1107.8
3.6	457.4	291.6	183.9	475.5	279.5	1212.4
3.8	514.7	331.5	187.4	518.9	289.8	1324.4
4.2	622.4	370.8	218.4	589.2	309.8	1521.6

TABLE III. Binding energy of neutron matter as function of the healing distance d, calculated with the Reid soft-core potential for $\rho = 0.8$ fm^{-3}.

d/r_0	E/N (MeV)	E_{LO}/N (MeV)
1.05	144.6	30.2
1.35	118.8	−2.3
2.0	115.2	−12.3
2.2	116.3	−12.9
2.5	125.6	−6.0

TABLE IV. Model energies for neutron matter calculated with the Reid soft-core potential.

ρ (fm^{-3})	ϵ_F (MeV)	ϵ_F^{mod} (MeV)	E/N (MeV)	E^{mod}/N (MeV)
0.2	40.7	41.3	20.0	21.1
1.0	119.0	124.1	165.1	172.4
1.2	134.4	127.2	214.1	210.5
1.4	137.5	137.6	271.4	275.5
1.6	162.8	146.3	336.5	341.0
1.8	176.1	157.7	406.0	411.5
3.0	247.5	191.6	914.5	921.1
4.2	309.8	225.7	1530.9	1521.3

TABLE V. Binding energy of neutron matter calculated with the Bressel-Kerman-Rouben potential.

ρ (fm^{-3})	$E_2^{(0)}$ (MeV)	$E_2^{(1)}$ (MeV)	T_3 (MeV)	E_{HO} (MeV)	ϵ_F (MeV)	E/N (MeV)
0.2	−20.1	−1.9	0.65	−1.3	40.7	19.3
0.4	−30.1	−1.9	3.2	1.4	64.6	35.9
0.6	−31.9	−1.2	10.4	9.2	84.7	62.0
0.8	−29.2	3.5	18.3	21.8	102.5	95.1
1.0	−24.7	12.3	26.7	39.0	119.0	133.3
1.2	−18.1	24.8	31.8	56.6	134.4	172.9
1.4	−7.5	39.7	43.4	83.2	148.9	224.6
1.6	4.0	59.4	55.6	115.0	162.8	281.8
1.8	18.3	79.7	61.5	141.1	176.1	335.5
2.0	35.7	106.8	59.4	166.2	188.9	390.8
2.2	55.3	130.0	65.8	195.8	201.3	452.4
2.6	106.7	181.6	64.3	245.8	225.0	577.5
3.0	167.5	230.3	53.6	283.9	247.5	698.9
3.4	255.1	262.8	44.3	307.1	269.1	831.3
3.8	359.4	286.2	28.9	315.1	289.8	964.3
4.2	474.7	286.6	17.5	304.1	309.8	1088.6

TABLE VI. Binding energy of neutron matter calculated with the Bethe-Johnson potential.

ρ (fm^{-3})	$E_2^{(0)}$ (MeV)	$E_2^{(1)}$ (MeV)	T_3 (MeV)	E_{HO} (MeV)	ϵ_F (MeV)	E/N (MeV)
0.6	5.2	1.3	19.0	20.3	84.7	107.8
0.8	29.8	11.8	32.2	44.0	102.5	171.3
1.0	61.0	28.6	48.6	77.2	119.0	248.5
1.2	87.2	42.9	63.0	105.9	134.4	327.5
1.4	129.7	64.9	79.7	144.6	148.9	423.2
1.6	175.7	89.3	97.6	187.4	162.8	525.9
1.8	227.4	115.8	115.9	231.8	176.1	635.3
2.0	285.0	152.6	129.5	282.1	188.9	756.0
2.2	349.3	181.8	149.9	331.7	201.3	882.3
2.4	411.0	207.4	172.8	380.4	213.3	1004.7
2.6	486.5	254.1	185.2	439.3	225.0	1150.8
2.8	558.5	276.7	211.5	488.2	236.4	1283.1
3.0	637.6	328.6	221.0	550.3	247.5	1435.4

TABLE VII. Model energies for neutron matter calculated with the Bethe-Johnson potential.

ρ (fm^{-3})	ϵ_F (MeV)	ϵ_F^{mod} (MeV)	E (MeV)	E^{mod}/N (MeV)
0.6	84.7	88.8	110.2	113.6
1.2	134.4	122.7	327.5	334.2
1.8	176.1	148.2	635.3	645.6
3.0	247.5	161.1	1435.5	1439.7

TABLE VIII. Binding energy of neutron matter calculated by the LOCV method with the V_1 potential.

ρ (fm^{-3})	E_2^{LOCV} (MeV)	ϵ_F (MeV)	d/r_0	E_{LOCV}/N (MeV)
0.2	58.9	40.7	1.30	99.6
0.4	160.5	64.6	1.24	225.1
0.6	291.1	84.7	1.26	375.8
0.8	444.4	102.5	1.26	546.9
1.0	616.1	119.0	1.27	735.1
1.4	1003.9	148.9	1.27	1152.8
1.8	1439.2	176.1	1.28	1615.3
2.2	1911.8	201.3	1.28	2113.1
2.6	2415.5	225.0	1.28	2640.5
3.0	2945.2	247.5	1.28	3192.7
3.4	3497.1	269.1	1.28	3766.2
3.8	4068.7	289.8	1.28	4358.5
4.2	4658.1	309.8	1.29	4967.9

TABLE IX. Binding energy of neutron matter calculated by the FHNC/0 method with the V_1 potential.

ρ (fm^{-3})	$E_2^{(0)}$ (MeV)	$E_2^{(1)}$ (MeV)	T_3 (MeV)	E_{HO} (MeV)	ϵ_F (MeV)	E/N (MeV)
0.2	59.6	11.7	1.8	13.5	40.7	113.8
0.4	131.2	37.8	12.1	49.9	64.6	245.7
0.6	208.1	70.9	39.6	110.5	84.7	403.3
0.8	309.1	110.8	60.4	171.2	102.5	582.8
1.0	420.4	157.3	81.8	239.1	119.0	778.5

TABLE X. Binding energy in MeV of neutron matter calculated with the V_1 potential. MC is obtained by Monte-Carlo calculations (Ref. 32), KR by Krotscheck (Ref. 33), FR by Fantoni and Rosati (Ref. 34), and Z by Zabolitky (Ref. 22) for different kinetic energy expressions.

ρ (fm^{-3})	MC E/N	KR E/N	FR E/N	E_{CW}	E_{JF}	Z E_{PB}	$\epsilon_F - \epsilon_{mod}$	E/N	$\epsilon_F - \epsilon_{mod}$
0.17	89			93	91	88	3		
0.2		105	112	112	109	105	4	113.8	
0.3	175			181	174	166	7		
0.4				257	247	234	9	245.7	
0.6		393	424	432	412	388	21	403.3	28.1
0.8				629	598	562	32	582.8	12.8
1.0	782	772	824	844	802	753	42	778.5	10.0

TABLE XI. Energy terms for neutron matter calculated with the V_1 potential.

ρ (fm^{-3})	E_{H1} (MeV)	$E_{H1,ex}$ (MeV)	$E_H - E_2^{(0)}$ (MeV)
0.2	11.3	−3.4	3.9
0.4	31.4	−9.0	15.4
0.6	46.8	−10.0	34.0
0.8	73.7	−16.1	53.2
1.0	107.2	−24.1	74.2

TABLE XIII. Binding energy of neutron matter as function of healing distance d, calculated with the V_1 potential for $\rho = 1.0$ fm^{-3}. $\Delta U = 0.1 U$.

d/r_0	E/N (MeV)	$E/N + \Delta U$ (MeV)
1.2	888.6	889.5
1.3	856.5	857.8
1.5	807.0	809.7
2.0	778.5	786.2
2.1	778.0	786.4

TABLE XII. Binding energy of neutron matter as function of healing distance d, calculated with the V_1 potential for $\rho = 0.8$ fm^{-3}.

d/r_0	$E_2^{(0)}$ (MeV)	T_3 (MeV)	E_{HO} (MeV)	E/N (MeV)
1.2	466	9	90	659
1.5	376	25	128	606
1.8	322	46	161	586
2.0	309	60	171	583
2.1	305	72	177	585

TABLE XIV. Model energies for neutron matter calculated with the V_1 potential.

ρ (fm^{-3})	ϵ_F (MeV)	ϵ_F^{mod} (MeV)	E/N (MeV)	E^{mod}/N (MeV)
0.2	40.7		113.8	118.4
0.6	84.7	112.8	403.3	411.5
0.8	102.5	115.3	582.8	595.7
1.0	119.0	129.0	778.5	795.0

NEUTRON MATTER CALCULATIONS BY THE FERMI- . . .

TABLE XV. Binding energy in MeV of neutron matter, calculated with the Reid soft-core potential for a healing distance $d \approx 1.2 r_0$.

ρ (fm^{-3})	$E_2^{(0)}$	$E_2^{(1)}$	T_3	E^{HO}	ϵ_F	E	d/r_0
0.6	−10.8	4.2	3.6	7.8	84.7	81.7	1.22
1.0	44.5	21.7	6.4	28.0	119.0	191.5	1.23
1.4	129.1	41.8	9.3	51.1	148.9	329.1	1.24
2.2	373.1	91.6	14.1	105.7	201.3	680.1	1.24
2.6	523.5	129.0	16.1	144.6	225.0	893.1	1.25
3.0	694.3	145.6	18.9	164.3	247.5	1106.1	1.25
3.4	868.3	185.8	20.1	205.9	269.1	1343.3	1.25
3.8	1062.0	190.2	22.3	212.4	289.8	1564.2	1.25

The integral equations (3.8) are solved by iteration, i.e., the scheme of calculation is

(1) set all G_{xy} equal to zero, i.e., $G_{xy}^{(0)} = 0$;

(2) calculate the functions (3.9) for $G_{xy}^{(0)} = 0$;

(3) calculate new $G_{xy} = G_{xy}^{(1)}$, i.e., the left-hand side of (3.8), using (5.10) and (5.11);

(4) set new $G_{xy}^{(2)} = \frac{1}{2}(G_{xy}^{(1)} + G_{xy}^{(0)})$;

(5) if $G_{xy}^{(2)} \neq G_{xy}^{(0)}$, continue the iteration process until convergence is obtained.

This method does not, however, always work for high densities. Then one may use, for instance, a Newton-Raphson iteration method.

The scheme of calculation becomes as shown in Fig. 2 for the FHNC/0 method, and the results are shown in Tables I—XIV and Figs. 3—12. In the tables and figures are given

$$E_2^{(0)} = (W + W_F)_{LO} ,$$

$$E_{LO} = E_2^{(0)} + \epsilon_F ,$$

$$E_2^{(1)} = (W + W_F) - (W + W_F)_{LO} ,$$

$$T_3 = U + U_F , \qquad (5.12)$$

$$E_{HO} = E_2^{(1)} + T_3 ,$$

$$E/N = E_2^{(0)} + E_{HO} + \epsilon_F .$$

In addition, E_H, E_{H1}, and $E_{H1,ex}$ are contributions from terms including H, H_1, and $H_{1,ex}$ functions defined in (3.13), and we also calculate model energies defined by[23]

$$E^{mod} = \langle \Phi | T | \Psi \rangle / \langle \Phi | \Psi \rangle + \langle \Phi | V | \Psi \rangle / \Phi | \Psi \rangle ,$$

$$\qquad (5.13)$$

$$\epsilon_F^{mod} = N^{-1} \langle \Phi | T | \Psi \rangle / \langle \Phi | \Psi \rangle .$$
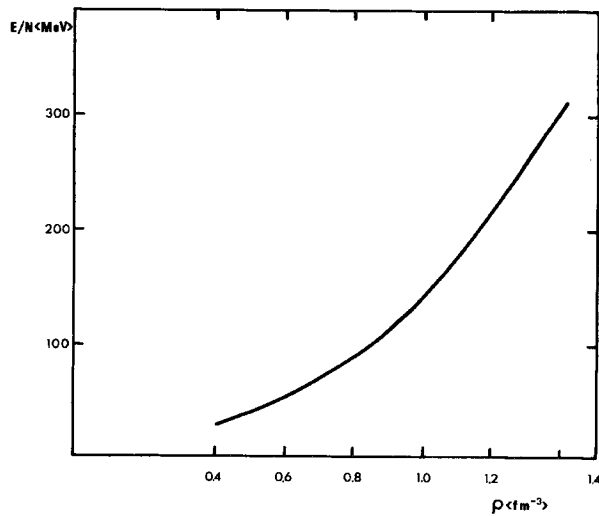

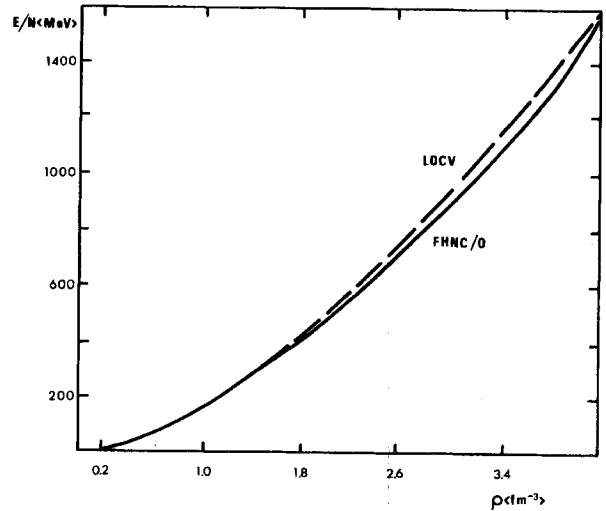FIG. 3. Binding energy of neutron matter calculated by the FHNC/0 method with the Hamada-Johnston potential.

FIG. 4. Binding energy of neutron matter calculated with the Reid soft-core potential.

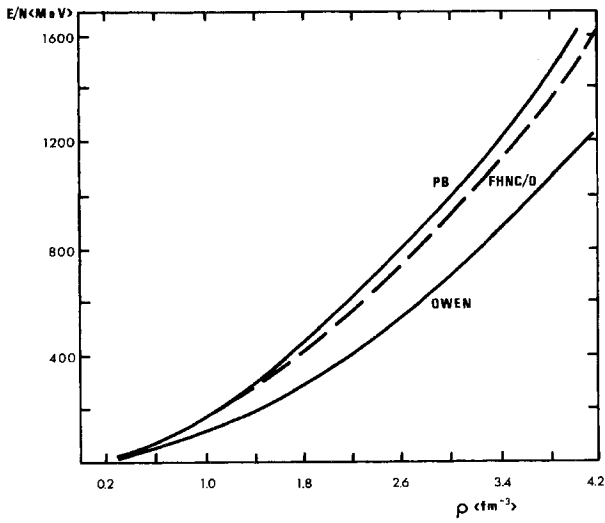**B. ARNTSEN AND E. ØSTGAARD**

FIG. 5. Binding energy of neutron matter calculated with the Reid soft-core potential by Pandharipande and Bethe (Ref. 6), the LOCV method of Owen *et al.* (Ref. 15), and our FHNC/0 method.
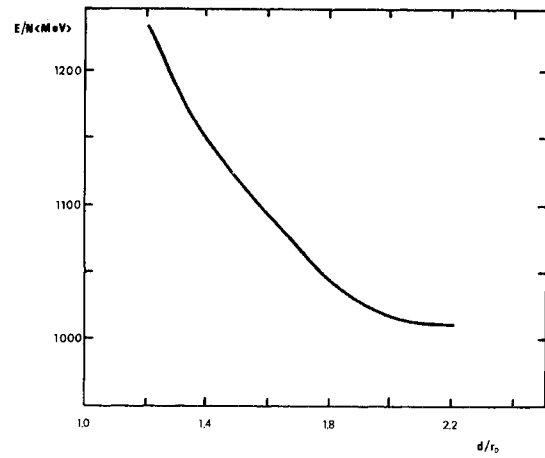

FIG. 7. Binding energy of neutron matter as function of the healing distance d, calculated by the FHNC/0 method with the Reid soft-core potential for $\rho = 3.2$ fm^{-3}.

$E_2^{(0)}$ then gives the energy when only the first (lowest order) term of the PS expansion is included, while E_{HO} gives the correction from the other (highest order) terms calculated in the FHNC/0 approximation. The model energies are calculated as a check on our method, i.e., E^{mod} and $\epsilon_F^{\mathrm{mod}}$ should be close to E and ϵ_F.

Results for the HJ potential are shown in Table I and Fig. 3, and we could not get numerical solutions of the FHNC equations for $\rho > 1.4$ fm^{-3}. The HJ potential has a hard core for $r < 0.49$ fm, and the free volume per particle becomes smaller and correlations between the particles more important than for the RSC and BJ potentials.

Results for the RSC potential are shown in Tables II—IV and Figs. 4—7. We see in Table II that T_3 becomes greater than $E_2^{(1)}$ for $\rho < 1.9$ fm^{-3}, since the RSC potential has a deep attractive well in the singlet-even state (V_0). Also, the contribution E_{H1} will cancel the contribution $E_{H1,\mathrm{ex}}$ for $\rho < 1.6$ fm^{-3} because of the

FIG. 6. Binding energy of neutron matter calculated by our FHNC/0 method with the Reid soft-core potential, and by Smith (Ref. 8) and Friedman and Pandharipande (Ref. 9) with noncentral tensor and spin terms included in the potentials and the correlation functions.
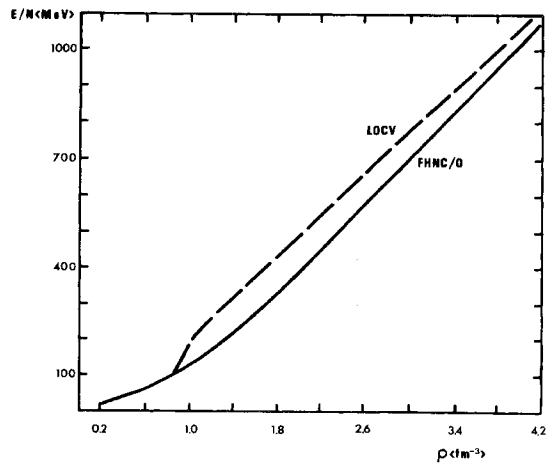

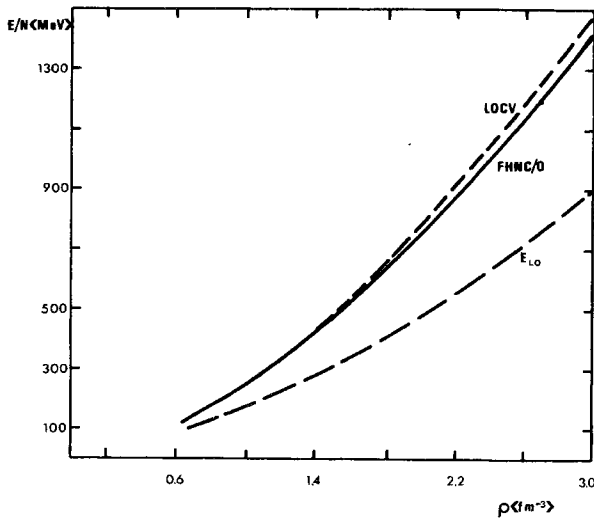FIG. 8. Binding energy of neutron matter calculated with the Bressel-Kerman-Rouben potential.

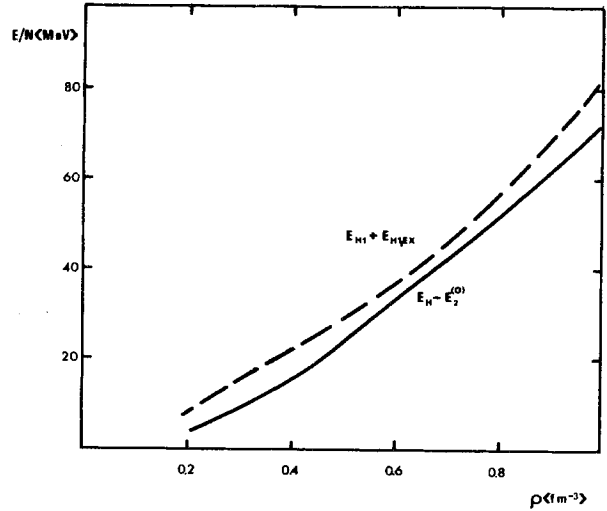FIG. 9. Binding energy of neutron matter calculated with the Bethe-Johnson potential.

FIG. 11. Energy contributions for neutron matter calculated by the FHNC/0 method with the V_1 potential.

triplet-odd potential (V_1). The choice of healing distance d is checked as in Table III and Fig. 5, and we see that we get a minimum for $d \approx 2r_0$. Model energies are shown in Table IV, and we see that the difference between ϵ_F and ϵ_F^{mod} is 10–30 %.

Results for the BKR potential are shown in Table V and Fig. 8. Here, it was not possible to obtain a healing distance $d = 2r_0$ for $f_2(r)$ for $\rho < 2.6$ fm^{-3}, i.e., we could not obtain the self-consistency condition, and we had to use the approximation

$$\lambda_2 f_2^2 = \lambda_0 f_0^2 . \tag{5.14}$$

The BKR potential has a rather "soft" core ($V = 670$ MeV for $r < 0.7$ fm), so the correlations between the particles will be correspondingly small, E_{HO} becomes less important compared to E, and T_3 decreases for increasing density. $E(\rho)$ finally becomes an almost linear function for the highest densities.

Results for the BJ potential are shown in Tables VI and VII and Fig. 9. We see from Table VI that correlations
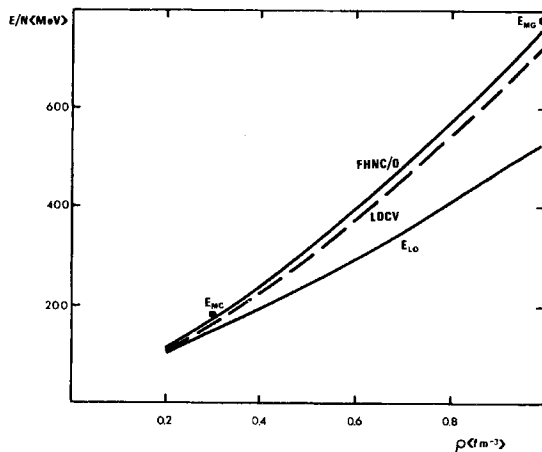

FIG. 10. Binding energy of neutron matter calculated with the V_1 potential. The circles labeled E_{MC} are obtained by Monte-Carlo calculations (Ref. 32).
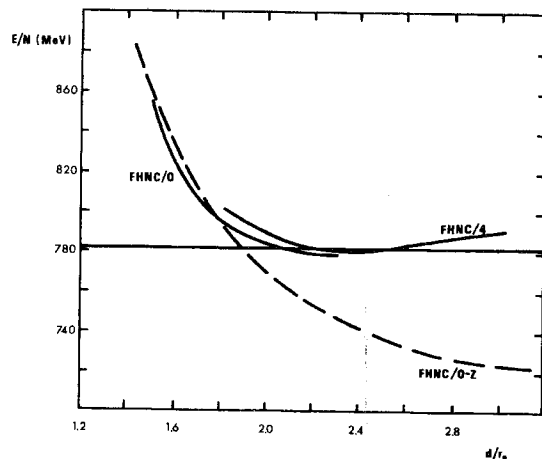

FIG. 12. Binding energy of neutron matter as function of the healing distance d, calculated with the V_1 potential for $\rho = 1.0$ fm^{-3}. The calculations FHNC/0—Z and FHNC/4—Z are done by Zabolitsky (Ref. 22). The straight line is obtained by Monte-Carlo calculations (Ref. 32).

between more than two particles are very important for large densities, and give approximately 40% contribution to the energy for $\rho \approx 3$ fm^{-3}. The three-body term T_3 is also approximately 40% of E_{HO} for the highest densities. Model energies are shown in Table VII, and we see that ϵ_F and ϵ_F^{mod} are very different for the highest densities.

Results for the V_1 potential are shown in Tables VIII—XIV and Figs. 10—12, since it is very convenient for studying the FHNC/0 method compared to the LOCV method, the various terms in (5.12) and (5.13), and the effects of the H functions in (3.13) and the healing distance d. We see from Table XII and Figs. 10 and 11, for instance, that the energy changes very little for $d > 2r_0$. We also see from Table XIII that E is quite close to E^{mod}, but there is a greater difference between ϵ_F and ϵ_F^{mod}.

VI. SUMMARY AND DISCUSSION

The energy per particle as function of density for the Hamada-Johnston and the Bethe-Johnson potentials are shown in Figs. 3 and 9, and Fig. 4 shows correspondingly results for the Reid soft-core potential together with the corresponding LOCV results. Figure 7 shows that the RSC energy, for instance, does not change very much when the healing distance is greater than $2r_0$.

In Fig. 8, a comparison between energy curves calculated by the LOCV method and the FHNC/0 method for the Bressel-Kerman-Rouben potential shows a rather different behavior for the two curves for $\rho > 0.8$ fm^{-3}. The sudden change in the energy predicted by the LOCV method at $\rho \approx 0.8$ fm^{-3} has earlier been interpreted as a phase transition[11,12] occurring when the repulsion from the soft core in the potential is not strong enough to keep the neutrons apart from each other. The FHNC/0 results show, however, that the energy increases smoothly with density, and such a phase transition will not occur.

Figures 10 and 12 show that our results for the V_1 potential are quite close to FHNC/4 results and Monte Carlo results. We also see that the energy changes very little with increasing healing distance for $d > 2r_0$. Tables IV and VII show model energies ϵ_F^{mod} and E^{mod}/N calculated for the Reid soft-core and the Bethe-Johnson potentials, which are in quite good agreement with energies shown in Figs. 4 and 9. Table XIV shows ϵ_F^{mod} and E^{mod}/N which are not too far from ϵ_F and E/N for the V_1 potential, and Table X also shows that our V_1 results are generally in good agreement with other calculations, even at high densities.

Figure 10 shows the energy per particle as function of density for the V_1 potential, and our results agree very well with results from Monte Carlo calculations.[32] A comparison with results obtained in the FHNC/4 approximation[22] is given in Fig. 12 for the V_1 potential and a particle density of $\rho = 1.0$ fm^{-3}. The FHNC/4 calculations and corresponding FHNC/0 calculations were made for a correlation function $f(r)$ obtained from Eqs. (3.2) and (3.4) in the limit $k_{av} \to 0$, i.e., they consider in effect a system of "bosons" interacting via the V_1 potential. The

healing distance d is then treated as a variational parameter and the energy $E(d)$ is varied numerically to give a minimum value. Since the boson-type correlation function could be quite different from the optimum correlation function, an upper bound to the energy is not obtained unless a massive partial summation of contributions or diagrams is performed. This is shown in Fig. 12, where the FHNC/0 calculations for the boson-type correlation function give results below the Monte Carlo results and the FHNC/4 results for large values of d.

In our calculations, a "true" fermion correlation function is used. And in addition, the healing distance d is not a true variational parameter, but simply a parameter introduced to improve the convergence of the cluster expansion. At the two-body level, as in the LOCV method, it is necessary to impose restrictions on the healing distance. When many-body contributions are included, however, the range of the correlation functions may be increased without problems for the convergence of the energy expansion.

It is important to try a large healing distance, since fermion systems should have an optimum correlation function which "goes" like $1 + \mathcal{O}(r^{-2})$ for $r \to \infty$.[35] And, in the limit $d \to \infty$, we should expect the energy to approach a correct limiting value if the wave function is close to the true wave function and the energy is evaluated correctly.

Since our correlation function is obtained at the two-body level and the FHNC/0 method is not exact, neither a correct value nor a true upper bound for the energy per particle will be obtained. Our FHNC/0 calculations, however, should be better than FHNC/0 calculations based on a boson-type correlation function.

From Table X we see that the FHNC/0 approximation seems to be reasonably accurate for state-independent correlation functions and Yukawa-type potentials for $d \lesssim 2r_0$ and $\rho \lesssim 2$ fm^{-3}. To permit an l-dependent correlation function, i.e.,

$$f_0 \neq f_1 = f_{odd\, l} \neq f_2 = f_{even\, l \neq 0} \; ,$$

we have used the approximations (3.3) and (3.5) in our calculations. The terms U and U_F could be rather sensitive to the choice of $f'_{av}(r)$, and one should possibly take a different $f'_{av}(r)$ in singlet and triplet states.[30,31]

We have neglected all noncentral components in the potentials. For most potentials this would only matter for the triplet-odd states, but we see from Fig. 6 that it could be important. Noncentral interactions seem to be able to reduce the energy for the Reid soft-core potential by almost 40% at high densities.[8,9]

To check the choice of healing distance in the LOCV method compared to the FHNC method, i.e., (3.14), we also calculated the energy by the FHNC/0 approximation for approximately the same healing distance as in the LOCV method. The results are shown in Table XV, and we find that E_{HO} is only 10% of E_{LO}. We also find, in general, that the results from LOCV calculations[25] are quite close to our FHNC/0 results.

*Present address: Petroleumsteknisk Forskningsinstitutt, 7034 Trondheim-NTH, Norway.

[1]K. A. Brueckner, J. L. Gammel, and J. T. Kubis, Phys. Rev. 118, 1095 (1960).

[2]M. Binder, R. H. Pierce, and M. Razavy, Can. J. Phys. 47, 2101 (1969).

[3]E. Østgaard, Nucl. Phys. A154, 202 (1970).

[4]P. J. Siemens and V. R. Pandharipande, Nucl. Phys. A173, 561 (1971).

[5]S. L. Schlenker and E. Lomon, Phys. Rev. C 3, 561 (1971).

[6]V. R. Pandharipande and H. A. Bethe, Phys. Rev. C 7, 1312 (1973).

[7]H. A. Bethe and M. B. Johnson, Nucl. Phys. A230, 1 (1974).

[8]R. A. Smith, Nucl. Phys. A328, 169 (1979).

[9]B. Friedman and V. R. Pandharipande, Nucl. Phys. A361, 502 (1981).

[10]R. Jastrow, Phys. Rev. 98, 1479 (1955).

[11]V. R. Pandharipande, Nucl. Phys. A174, 641 (1971).

[12]V. R. Pandharipande, Nucl. Phys. A178, 123 (1971).

[13]M. Miller, C. W. Woo, J. W. Clark, and W. J. ter Louw, Nucl. Phys. A184, 1 (1972).

[14]O. Benhar, C. Ciofi Degli Atti, A. Kallio, L. Lantto, and P. Toropainen, Phys. Lett. 60B, 129 (1976).

[15]J. C. Owen, R. F. Bishop, and J. M. Irvine, Ann. Phys. (N.Y.) 102, 170 (1976).

[16]D. A. Chakkalakal, C. H. Yang, and J. W. Clark, Nucl. Phys. A271, 185 (1976).

[17]E. Lunnan and E. Østgaard, Physica (Utrecht) 101B, 22 (1980).

[18]L. Shen and C. W. Woo, Phys. Rev. D 10, 371 (1974).

[19]J. M. J. van Leeuwen, J. Groeneveld, and J. de Boer, Physica (Utrecht) 25, 792 (1959).

[20]E. Krotscheck and M. L. Ristig, Nucl. Phys. A242, 389 (1975).

[21]S. Fantoni and S. Rosati, Nuovo Cimento 25A, 523 (1975).

[22]J. G. Zabolitzky, Phys. Rev. A 16, 1258 (1977).

[23]B. Arntsen and E. Østgaard, Ark. Fys. 10 (1983).

[24]L. J. Lantto and P. J. Siemens, Nucl. Phys. A317, 55 (1979).

[25]O. Forseth and E. Østgaard, Phys. Scr. 24, 519 (1981).

[26]T. Hamada and I. D. Johnston, Nucl. Phys. 34, 382 (1962).

[27]V. R. Pandharipande, Nucl. Phys. A181, 33 (1972).

[28]R. V. Reid, Ann. Phys. (N.Y.) 50, 411 (1968).

[29]C. N. Bressel, A. K. Kerman, and B. Rouben, Nucl. Phys. A124, 624 (1969).

[30]J. C. Owen, Ann. Phys. (N.Y.) 118, 373 (1979).

[31]I. E. Lagaris, V. R. Pandharipande, and R. B. Wiringa, Nucl. Phys. A328, 113 (1979).

[32]C. Ceperley, G. V. Chester, and M. H. Kalos, Phys. Rev. B 16, 308 (1977).

[33]E. Krotscheck, Nucl. Phys. A317, 149 (1979).

[34]S. Fantoni and S. Rosati, Lett. Nuovo Cimento 16, 531 (1976).

[35]E. Krotscheck, Phys. Rev. A 15, 397 (1977).